International Journal of Smart Electrical Engineering, Vol.7, No.4, Fall 2018 *ISSN: 2251-9246*
EISSN: 2345-6221
pp. 138:144

Optimal Scheduling of CHP-based Microgrid Under Real-Time Demand Response Program

Hamed Pashaei-Didani*[1], Kazem Zare[1] , Sayyad Nojavan[2]

[1] Faculty of Electrical and Computer Engineering, University of Tabriz, Tabriz, Iran, h.pashaei96@ms.tabrizu.ac.ir,
[2] Department of Electrical Engineering, University of Bonab, Bonab, Iran, sayyad.nojavan@bonabu.ac

Abstract

Microgrid (MG) is considered as a feasible solution to integrate the distributed energy sources. In this paper, optimal scheduling of a grid-connected MG is investigated considering different power sources as combined heat and power (CHP) units, only power and heat generating units, and battery storage systems. Two different feasible operating regions are considered for the CHP units. In addition, heat buffer tank and the CHP units are used to meet heat demand of the MG. In order to investigate the impact of demand response programs on the optimal scheduling of the MG, time-of-use (TOU) and real-time pricing (RTP) rates of demand response programs (DRP) are implemented. To do so, the problem is solved in three case studies as RTP-DRP, TOU-DRP, and without DRP. Based on the obtained results, total energy procumbent cost of the MG is reduced about 2.54% and 6.66% after applying the TOU and RTP demand response programs in comparison with the without DRP case., respectively. The problem is formulated as MILP and solved under CLPX solver in the GAMS software.

Keywords: microgrid; demad response program; time-of-use rate; real-time pricing; combined heat and power units.

Article history: Received 10-Oct-2018; Revised 08-Nov-2018; Accepted 28-Nov-2018.

1. Introduction

Microgrid (MG) is defined as a cluster of loads and distributed energy resources (DERs), which may include wind turbines, photovoltaic systems, and energy storage systems (EESs) etc. [1]. The concept of MG can be considered as an effective tool for integration of distributed dispatchable generators and energy storage devices in current power systems [2].

A) Literature review

Optimal scheduling of an MG is studied and investigated by considering different issues. Energy management of an MG is pursued by using artificial intelligence techniques based on the generalized formulation in [3]. A new method based on the improved real-coded genetic algorithm and enhanced mixed integer linear programming is proposed to unit commitment and economic dispatch of MG units in [4]. Scheduling power sources in a typical MG, in the presence of electric vehicles, is investigated in [5]. Optimal dispatch of MG's generating units is studied in [6],[7], by taking cost and emission into account and defining the multi-objective function. The non-dominated sorting genetic algorithm II is used for the optimal scheduling of ESSs in MG to deal with the multi-objective optimization problem in [8]. By minimizing energy costs, pollutant emissions, and maximizing penetration of renewable energy, green energy management investigated in [9].

Combined heat and power (CHP) units can be used in MG in order to reduce thermal energy generation cost. CHP units can provide heat and power at the same time by using wasted heat in power generation process [10]. Economic dispatch problem of CHP-based MG is well studied in [11],[12].

As an effective tool to reduce operating cost, demand response programs (DRP) can be used in MG scheduling problem [13]. According to US Department of Energy, DRPs is defined as changes in end-user clients' electric consumption patterns in reaction to electricity price changes over time or to incentive the consumers to decrease the compensations at peak periods or when the system reliability problems occur [14]. Integration of renewable energy resources such as wind power, solar, small hydro, biomass and CHP is presented in [15] in the presence of DRPs. The pricing and operation strategy for a retailer in the presence of DRP are investigated in [16].

B) Novelty and contributions

In this paper, scheduling of CHP-based MG is pursued the presence of DRPs such as real-time-pricing (RTP) and time-of-use (TOU). Different generation unit as CHP, power-only unit, heat only unit, heat buffer tank, and storage is considered to supply load demand. The impact of TOU and RTP is investigated and compared with the without DRP case.

C) Paper organization

The rest of this paper is organized as follows: model of MG components and DRPs are presented in Section II. The simulation method is introduced in Section III. Section IV provides the information of the case study. Finally, the paper is concluded in Section V.

2. Problem Formulation

The considered MG model contains two CHP units, battery storage system, power and heat only units, and heat buffer tank. In this work, optimal power is investigated by taking total cost as the objective variable. DRPs are considered to flatten the load curve and reduce demand at high price periods, which will result reduction in the operating cost of the MG.

A) Objective Function

Total operating cost is defined as objective function (1) including a set of terms such as the cost of purchased power from the grid, operating cost of units, degradation cost of storage, and revenue of selling power to the grid [17].

$$OF=\sum_{h=1}^{24}\left\{\begin{array}{l}\lambda_h\times P_h^{G,buy}+\sum_{i=1}^{N_{CHP}}C(P_{i,h}^{CHP},H_{i,h}^{CHP})+\\ C(\mathrm{P}_h^{PO})+C(\mathrm{H}_h^{PO})+\\ \sum_{j\in CHP,\mathrm{PO,b}}(C_{j,SU}\,SU_h^j+C_{j,SD}\,SD_h^j)+\\ C_k^{\deg}(\sum_{k=1}^{N_k}\frac{P_{k,h}^{disc}}{\eta_k^{disc}}+\eta_k^C\times P_{k,h}^C)-\lambda_h\times P_h^{G,sell}\end{array}\right\} \quad (1)$$

where λ_h, is the price of power at time h in (\$/MWh), $P_h^{G,sell}$ / $P_h^{G,buy}$ is the amount of electricity sold/bought to/from the network at time h (MWh), $C(P_{i,h}^{CHP},H_{i,h}^{CHP})$, $C(\mathrm{P}_h^{PO})$, and $C(\mathrm{H}_h^{PO})$ are the CHP, power only, heat only units cost function, respectively, $C_{j,SU}$ and $C_{j,SD}$ are startup/shutdown cost of generation facility in \$ respectively, SU_h^j and SD_h^j are binary variables of start-up and shut-down status for the units at time h, $C_k^{\deg}$ is cost for battery degradation in \$/kWh, $P_{k,h}^C$ and $P_{k,h}^{disc}$ are charge and discharging power of battery in kW respectively.

B) Power balance

With consideration of DRPs, generated power should meet the load demand at each hour [18]. This issue is expressed in Eq. (2).

$$P_h^{G,buy}-P_h^{G,\mathrm{sell}}+P_h^{PO}+P_h^{disc}-P_h^C-P_h^{DR}+\sum_{i=1}^{N_{CHP}}P_{i,h}^{CHP}=0;\forall h \quad (2)$$

where P_h^{DR}, is the electric load demand after applying DR program at h.th load level.

C) CHP unit's model

Two types of CHP units are considered in the MG model which each unit has different feasible operating regions (FORs). The first type of CHPs is characterized by Eqs. (2)-(7) [4].

$$P_{i,\mathrm{h}}^{CHP}-P_{i,\mathrm{A}}^{CHP}-\frac{P_{i,\mathrm{A}}^{CHP}-P_{i,\mathrm{B}}^{CHP}}{H_{i,\mathrm{A}}^{CHP}-H_{i,\mathrm{B}}^{CHP}}(H_{i,\mathrm{h}}^{CHP}-H_{i,\mathrm{A}}^{CHP})\le 0 \quad (3)$$

$$P_{i,\mathrm{h}}^{CHP}-P_{i,B}^{CHP}-\frac{P_{i,B}^{CHP}-P_{i,C}^{CHP}}{H_{i,B}^{CHP}-H_{i,C}^{CHP}}(H_{i,\mathrm{h}}^{CHP}-H_{i,B}^{CHP})\ge -(1-\mathrm{V}_{i,h}^{CHP})\times M \quad (4)$$

$$P_{i,\mathrm{h}}^{CHP}-P_{i,C}^{CHP}-\frac{P_{i,C}^{CHP}-P_{i,\mathrm{D}}^{CHP}}{H_{i,\mathrm{C}}^{CHP}-H_{i,\mathrm{D}}^{CHP}}(H_{i,\mathrm{h}}^{CHP}-H_{i,\mathrm{C}}^{CHP})\ge -(1-\mathrm{V}_{i,h}^{CHP})\times M \quad (5)$$

$$0\le P_{i,h}^{CHP}\le P_{i,A}^{CHP}\times V_{i,h}^{CHP} \quad (6)$$

$$0\le H_{i,h}^{CHP}\le H_{i,B}^{CHP}\times V_{i,h}^{CHP} \quad (7)$$

According to [19], the FOR of the second type of CHP is characterized by Eq. (8)-(16). In order to apply conventional formulation, the gray region (FEG) would not be considered. Therefore, this area is divided into two sub-section as sub-section I and II, using binary variables $X_{1,\mathrm{h}}$ and $X_{2,\mathrm{h}}$.

$$P_{i,\mathrm{h}}^{CHP}-P_{i,\mathrm{B}}^{CHP}-\frac{P_{i,\mathrm{B}}^{CHP}-P_{i,C}^{CHP}}{H_{i,B}^{CHP}-H_{i,C}^{CHP}}(H_{i,\mathrm{h}}^{CHP}-H_{i,B}^{CHP})\le 0 \quad (8)$$

$$P_{i,\mathrm{h}}^{CHP}-P_{i,C}^{CHP}-\frac{P_{i,C}^{CHP}-P_{i,D}^{CHP}}{H_{i,C}^{CHP}-H_{i,D}^{CHP}}(H_{i,\mathrm{h}}^{CHP}-H_{i,C}^{CHP})\le 0 \quad (9)$$

$$P_{i,\mathrm{h}}^{CHP} - P_{i,\mathrm{E}}^{CHP} - \frac{P_{i,\mathrm{E}}^{CHP} - P_{i,\mathrm{F}}^{CHP}}{H_{i,\mathrm{E}}^{CHP} - H_{i,\mathrm{F}}^{CHP}}(H_{i,\mathrm{h}}^{CHP} - H_{i,\mathrm{E}}^{CHP}) \geq -(1 - X_{1,h}) \times M \quad (10)$$

$$P_{i,\mathrm{h}}^{CHP} - P_{i,D}^{CHP} - \frac{P_{i,D}^{CHP} - P_{i,E}^{CHP}}{H_{i,\mathrm{D}}^{CHP} - H_{i,\mathrm{E}}^{CHP}}(H_{i,\mathrm{h}}^{CHP} - H_{i,D}^{CHP}) \geq -(1 - X_{2,h}) \times M \quad (11)$$

$$0 \leq P_{i,h}^{CHP} \leq P_{i,A}^{CHP} \times V_{i,\mathrm{h}}^{CHP} \quad (12)$$

$$0 \leq H_{i,h}^{CHP} \leq H_{i,\mathrm{C}}^{CHP} \times V_{i,h}^{CHP} \quad (13)$$

$$X_{1,h} + X_{2,h} = V_{i,h}^{CHP} \quad (14)$$

$$H_{i,h}^{CHP} - H_{i,E}^{CHP} \leq (1 - X_{1,h}) \times M \quad (15)$$

$$H_{i,h}^{CHP} - H_{i,E}^{CHP} \leq -(1 - X_{2,h}) \times M \quad (16)$$

Each of the abovementioned equations, describes some part of the FOR in the second type of CHP units.

Total operation cost of a CHP is modeled by Eq. (17) as presented in [20].

$$C(P_h^{CHP}, H_h^{CHP}) = \mathrm{a} \times (\mathrm{P}_h^{CHP})^2 + b \times P_h^{CHP} + c + d \times (H_h^{CHP})^2 + e \times H_h^{CHP} + f \times H_h^{CHP} \times P_h^{CHP} \quad (17)$$

where a, b, c, d, e and f are cost function coefficients of CHP units.

D) Power-only and heat-only model

Operation constraints of power-only and heat-only units are presented by Eq. (18) and Eq. (19).

$$P_h^{PO-\min} \times V_h^{PO} \leq P_h^{PO} \leq P_h^{PO-\max} \times V_h^{PO} \quad (18)$$

$$H_h^{b-\min} \times V_h^{b} \leq H_h^{b} \leq H_h^{b-\max} \times V_h^{b} \quad (19)$$

Eq. (20) and Eq. (21) describe the cost functions of power-only and heat only units.

$$C(P_h^{PO}) = \lambda_{PO} \times P_h^{PO} \quad (20)$$

$$C(H_h^{b}) = \lambda_b \times H_h^{b} \quad (21)$$

E) Electrical energy storage model

Charge and discharge limits are imposed by Eq. (22) and Eq. (23) [21].

$$0 \leq P_h^{c} \leq b_h^{c} \times P_h^{c,\max}, \quad 0 \leq P_h^{disc} \leq b_h^{disc} \times P_h^{disc,\max} \quad (22)$$

$$E_k^{\min} \leq E_{h,s} \leq E_k^{\max} \quad (23)$$

where b_h^c and b_h^{disc} are binary variables of charging/discharging state, $E_{h,s}$ is the capacity of the battery (kWh), $E_k^{\min} / E_k^{\max}$ is minimum/maximum energy stored in the battery (kWh). Eq. (24) is applied to avoid charging and discharging at the same time.

$$b_h^{c} + b_h^{disc} \leq 1, \ \ b_h^{c}, b_h^{disc} \in \{1,0\} \quad (24)$$

The dynamic energy model of the battery is stated by Eq. (25).

$$E_{h+1} = E_h + (\eta^c \times P_h^c - \frac{P_h^{disc}}{\eta^{disc}}) \quad (25)$$

F) Heat buffer tank

The heat buffer tank is used for heat storage and modeled based on [20]. The total generated heat is calculated by Eq. (26).

$$\bar{H}_h = \sum_{i=1}^{N_{CHP}} H_{i,h}^{CHP} + H_h^{b} \quad (26)$$

By using $\beta_{gain} / \beta_{loss}$ which are heat generation loss/excess for the CHP unit during startup/shutdown period, heat losses can be modeled as Eq. (27).

$$H_h = \bar{H}_h - \beta_{loss} . SU_h^i + \beta_{gain} . SD_h^i; \ i \in CHP \quad (27)$$

The available heat capacity in each time interval in the heat buffer tank B_h is expressed as Eq. (28).

$$B_h = (1 - \eta) \times B_{h-1} + H_h - \bar{H}_h^{load} \quad (28)$$

where η is heat loss rate for the heat buffer tank.

By using Eq. (29), the maximum available capacity of heat storage can be limited.

$$B_{\min} \leq B_h \leq B_{\max} \quad (29)$$

where $B_{\min} / B_{\max}$, is minimum/maximum heat buffer tank capacity in MW.

Equation (30) and (31) are applied to model the ramping up/down rates for the heat storage system.

$$B_h - B_{h-1} \leq B_{\max}^{ch\arg e} \quad (30)$$

$$B_{h-1} - B_h \leq B_{\max}^{disch\arg e} \quad (31)$$

where $B_{\max}^{ch\arg e} / B_{\max}^{disch\arg e}$ is the maximum charge/discharge rate of the storage MWth.

G) Startup and shutdown status

The startup and shutdown status of each unit can be modeled by Eq. (32) and Eq. (33).

$$SU_h^i = V_h^i \times (1 - V_{h-1}^i), \ \ i \in CHP, PO \quad (32)$$

$$SD_h^i = (1 - V_h^i) \times V_{h-1}^i, \ i \in CHP, PO \quad (33)$$

H) Electric load with demand response

By applying DR programs load is transferred from high price periods to low price periods which according to [22] will avoid unnecessary capital investments and costly energy procurement. In this paper, TOU and RTP are applied to show their impact on final results.

– *TOU-DR formulation*

TOU-DRP is one the most important and common used DRPs, which is formulated by Eq. (34) [23].

$$P_h^{DR} = P_h^{D} + ldr_h \quad (34)$$

where ldr_h is the shifted load from another load level to the h.th load level. ldr_h is calculated by using Eq. (35).

$$ldr_h = DR_h \times P_h^D \tag{35}$$

where DR_h is the participation factor of the load in the DRP at h.th load level and P_h^D is the base electric load at h.th load level in MWh.

As expressed in Eq. (36), the total shifted load over the period is assumed to be zero [24].

$$\sum_{h=1}^{24} ldr_h = 0 \tag{36}$$

Note that the DR_h should be limited at each time period, which is shown in Eq. (37).

$$DR_h^{\min} \le DR_h \le DR_h^{\max} \tag{37}$$

In this paper $DR_h^{\min}$ is assumed to be equal -30% and $DR_h^{\max}$ to be equal +30%.

I) RTP-DR programing

The RTP model is developed according to the predicted data for electricity demand and this model will be used to implement the demand response program.

$$T_d = \sum_{h=1}^{24} P_h^D \tag{38}$$

In Eq. (38), T_d is the total load demand of the MG. Thereby, the average electricity demand, P_{av} , can be formulated as Eq. (39).

$$P_{av} = \frac{T_d}{24} \tag{39}$$

The float factor of RTP, γ_h , can be considered as Eq. (40).

$$\gamma_h = \frac{P_h^D}{P_{av}} \tag{40}$$

The RTP model can be expressed as follows:

$$\lambda_{RTP} = \gamma_h . \lambda_{TOU} \tag{41}$$

$$\lambda_{RTP}^{Min} \le \lambda_{RTP} \le \lambda_{RTP}^{Max} \tag{42}$$

where λ_{TOU} is the benchmark price which is the time-of-use pricing in this paper. λ_{RTP}^{Min} and λ_{RTP}^{Max} are the minimum and maximum limits of the RTP, respectively.

With considering the RTP of DRP, the load demand can be formulated as Eq. (43).

$$\lambda_{RTP} = \gamma_h . \lambda_{TOU} \tag{43}$$

$$\lambda_{RTP}^{Min} \le \lambda_{RTP} \le \lambda_{RTP}^{Max} \tag{44}$$

where the E is the demand-price elasticity coefficient. It should be denoted that E is determined by analyzing the customer types and historical demand data. According to [20], E can take values in the interval [-0.5, 0]. In this paper, the E is considered equal to - 0.5.

3. Solution Method

In this paper, the optimal scheduling problem of a MG is formulated as mixed integer linear programming to minimize the total energy procurement cost of the MG. the problem is solve under CLPX solver in the GAMS optimization software.

4. Case Study

A) Input data

All the required information for the simulation such as base load, CHP units coefficients etc. are derived from [1].

B) Simulation Result

As said before, by applying demand response programs the load is shifted from peak periods to off-peak periods. According to the obtained results, total cost of energy precedent of the MG is equal to \$5,088.077, \$4,958.927, and \$4,749.380 for without DRP, TOU-DRP, and RTP-DRP, respectively. It is obvious that by applying DRPs the total cost is reduced. By applying TOU-DRP, 2.54% reduction in the total energy procurement cost of the MG is achieved. In addition, the RTP-TOU has reduced procurement cost about 6.66%. Base on the abovementioned descriptions, by implementing the RTP better results can be obtained in comparison with the TOU-DRP. A summary of the obtained results are presented in TABLE I. The load profile under RTP and TOU rates of DRP is depicted in Fig. 1. It is obvious that the load profile is more flattened under RTP-DRP. Also, it should be noted that shifted load in the TOU-DRP is limited on 30% of the base load.

Exchanged power between the MG and upstream grid is illustrated in Fig. 2 for considered case studies. Note that at each hour, procured power from the grid is presented by positive values while negative values present sold power to the grid. As it can be seen, 2.091, 3.158, and 1.988 MW are the maximum purchased power from the grid for RTP-TOU, TOU-DRP, and without DRP cases recorded at hours 2, 22, and 22, respectively. In addition, the maximum sold power to the grid are reported as 1.199, 2.598, and 2.526 MW for RTP-TOU, TOU-DRP, and without DRP cases, respectively. Fig. 3 illustrates the power production of the CHP units in the considered three cases. Obtained results show the produced power by the CHPs is same in RTP-DRP and without DRP cases. The maximum produced power by the CHP units is equal to 3.408 MW in all cases. Also, the minimum amount of generated power of the CHP in RTP-

DRP is obtained as 0.4 MW while this number is equal to 1.792 MW in RTP-DRP and without DRP cases. Heat generation of the CHP units is presented in Fig. 4. As said before, heat and power generation of CHP units are dependent to each hour. Therefore, as was expected, heat generation of the CHP units is same for TOU-DRP and without DRP cases. It should be noted that produced heat by the CHP is used to meet heat demand of the MG.

The power production of the power-only unit, which is considered to meet power demand of the MG, is depicted in Fig. 5. Note that the maximum capacity of the MG is equal to 1 MW. The production of the power-only unit is in accordance with the load profile and power price.

Table.1.
Summery of obtained results

Case study	*Total cost ($)*	*Cost reduction due to DRP (%)*
Without DRP	5,088.077	----
TOU-DRP	4,958.927	2.54
RTP-DRP	4,749.380	6.6

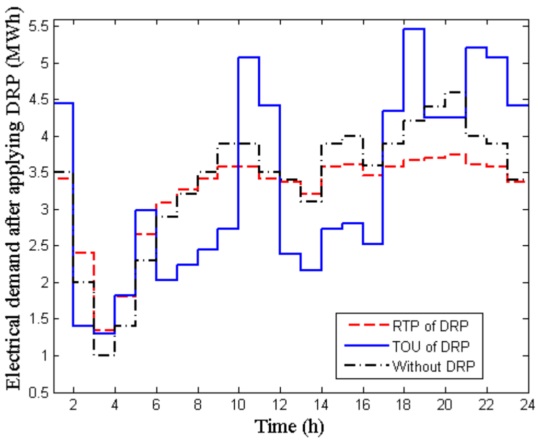

Fig. 1. The Load demand after applying demand response programs

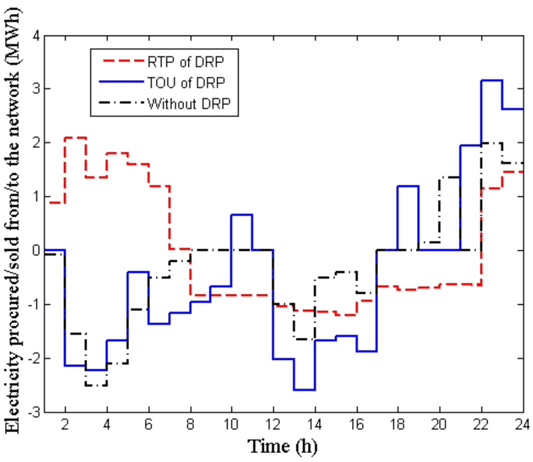

Fig. 2. Exchanged power with the MG and upstream grid

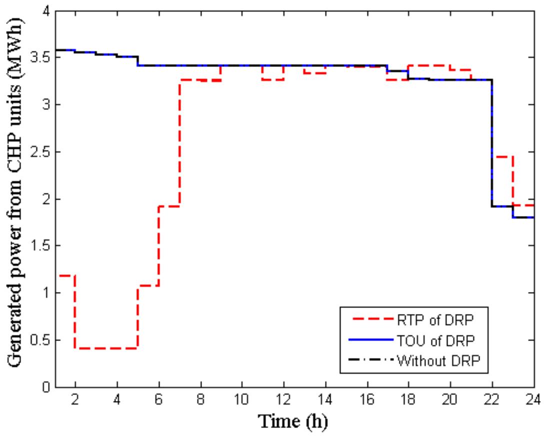

Fig. 3. Generated power by the CHP units

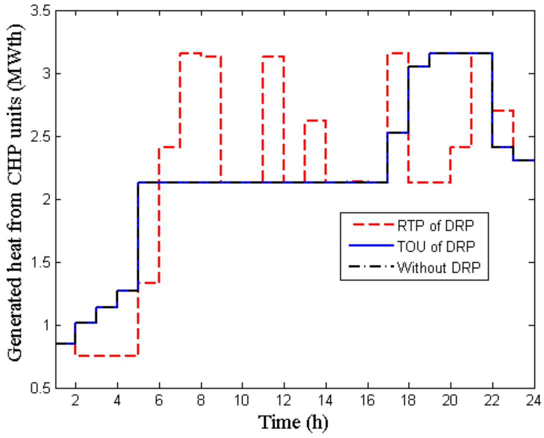

Fig. 4. Generated power by the CHP units

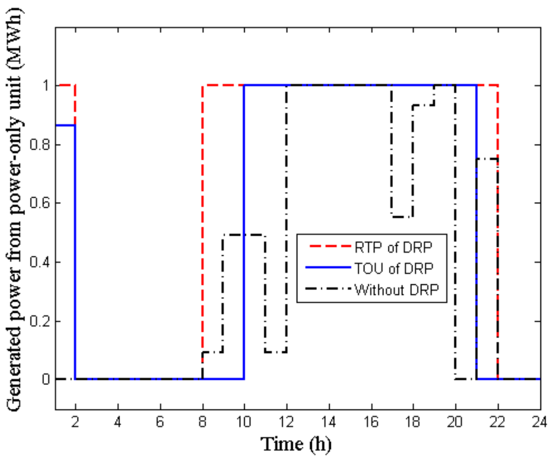

Fig. 5. Generated power by the power-only unit

The battery storage system is used to store electricity power during the off-peak period and use stored energy during the peak periods. The stored energy in the battery storage system is depicted in Fig 6. As was expected, the battery is discharged at peak load demand periods in the considered cases.

Figure 7 depicts the charging or discharging states of the battery during 24-hour for the three case studies. It should be noted that positive values show charged power and negative values present the discharged power. According to the Fig. 7, in the RTP-TOU, the battery is charged during hours 2-4 and discharged during hours 1 and 14-15. In addition, in the other cases the battery is discharged at hour 14.

The heat buffer tank is considered to meet the heat demand of the MG. available heat energy in the heat buffer tank is depicted in Fig. 8 for three cases in the time horizon of the study. The maximum stored energy in the heat buffer tank is equal to 4 MWth for TOU-DRP and without DRP cases. In the RTP-DRP, the maximum and minimum stored energy are recorded as 3.921 and 0 MWth.

5. Conclusion

In this paper, the short-term scheduling of a CHP-based MG is investigated under demand response programs. In order to assess the impact of demand response programs on the scheduling of the MG, time-of-use and real-time pricing rates of demand response programs are implemented and the problem is solve in three cases as with TOU-DRP, RTP-DRP, and without DRP. By applying demand response programs the load is shifted from peak periods to off-peak periods which result reduction in total energy procurement cost. According to the obtained results, total cost of energy precedent of the MG is equal to $5,088.077, $4,958.927, and $4,749.380 for without DRP, TOU-DRP, and RTP-DRP, respectively. Based on the abovementioned results, 2.54% and 6.66% reduction is obtained by applying TOU-DRP and RTP-TOU, respectively. The operation of the different generating units of the MG is analyzed in the three case studies for the time horizon of the study.

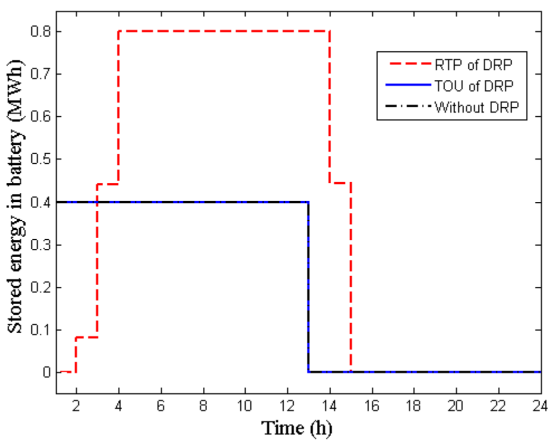

Fig. 6. Stored energy in the battery storage system

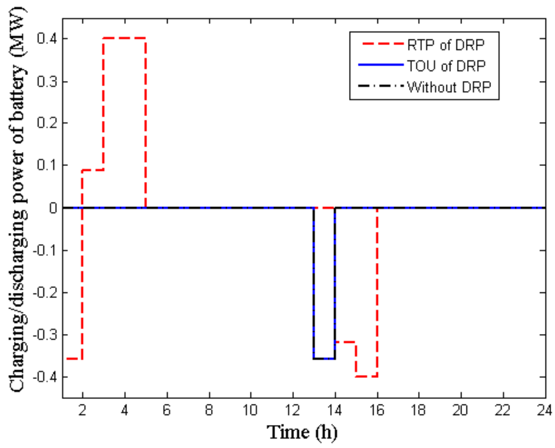

Fig. 7. Charging/discharging state of the battery storage system

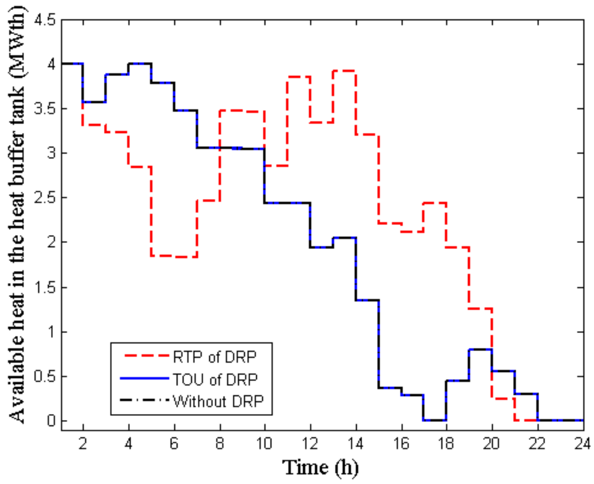

Fig. 8. Available heat in the heat buffer tank

References

[1] M. Nazari-Heris, S. Abapour, and B. Mohammadi-Ivatloo, “Optimal economic dispatch of FC-CHP based heat and power micro-grids,” Appl. Therm. Eng., Vol. 114 , Mar. 2017.

[2] Z. Luo, Z. Wu, Z. Li, H. Cai, B. Li, and W. Gu, “A two-stage optimization and control for CCHP microgrid energy management,” Appl. Therm. Eng., Vol. 125. 2017.

[3] A. Chaouachi, R. M. Kamel, R. Andoulsi, and K. Nagasaka, “Multiobjective Intelligent Energy Management for a Microgrid,” IEEE Trans. Ind. Electron., Vol. 60, No. 4. 2013.

[4] B. Mohammadi-Ivatloo, M. Moradi-Dalvand, and A. Rabiee, “Combined heat and power economic dispatch problem solution using particle swarm optimization with time varying acceleration coefficients,” Electr. Power Syst. Res., Vol. 95, 2013.

[5] B. Khorramdel, H. Khorramdel, J. Aghaei, A. Heidari, and V. G. Agelidis, “Voltage Security Considerations in Optimal Operation of BEVs/PHEVs Integrated Microgrids,” IEEE Trans. Smart Grid, Vol. 6, No. 4, 2015.

[6] M. Di Somma et al., “Multi-objective design optimization of distributed energy systems through cost and exergy assessments,” Appl. Energy, Vol. 204, 2017.

[7] Z. Li and Y. Xu, “Optimal coordinated energy

dispatch of a multi-energy microgrid in grid-connected and islanded modes," Appl. Energy, Vol. 210, 2018.

[8] C. Wang, Y. Liu, X. Li, L. Guo, L. Qiao, and H. Lu, "Energy management system for stand-alone diesel-wind-biomass microgrid with energy storage system," Energy, Vol. 97, 2016.

[9] M. Elsied, A. Oukaour, H. Gualous, and R. Hassan, "Energy management and optimization in microgrid system based on green energy," Energy, Vol. 84, 2015.

[10] X. P. Chen, N. Hewitt, Z. T. Li, Q. M. Wu, X. Yuan, and T. Roskilly, "Dynamic programming for optimal operation of a biofuel micro CHP-HES system," Appl. Energy, Vol. 208, 2017.

[11] M. Nemati, M. Braun, and S. Tenbohlen, "Optimization of unit commitment and economic dispatch in microgrids based on genetic algorithm and mixed integer linear programming," Appl. Energy, Vol. 210,. 2018.

[12] M. Alipour, K. Zare, and B. Mohammadi-Ivatloo, "Short-term scheduling of combined heat and power generation units in the presence of demand response programs," Energy, Vol. 71, 2014.

[13] S. Nojavan, K. Zare, and B. Mohammadi-Ivatloo, "Risk-based framework for supplying electricity from renewable generation-owning retailers to price-sensitive customers using information gap decision theory," Int. J. Electr. Power Energy Syst., Vol. 93, 2017.

[14] H. A. Aalami, H. Pashaei-Didani, and S. Nojavan, "Deriving nonlinear models for incentive-based demand response programs," Int. J. Electr. Power Energy Syst., Vol. 106, 2019.

[15] L. Montuori, M. Alcázar-Ortega, C. Álvarez-Bel, and A. Domijan, "Integration of renewable energy in microgrids coordinated with demand response resources: Economic evaluation of a biomass gasification plant by Homer Simulator," Appl. Energy, Vol. 132, 2014.

[16] S. Nojavan, R. Nourollahi, H. Pashaei-Didani, and K. Zare, "Uncertainty-based electricity procurement by retailer using robust optimization approach in the presence of demand response exchange," Int. J. Electr. Power Energy Syst., Vol. 105,. 2019.

[17] S. Nojavan, A. Najafi-Ghalelou, M. Majidi, and K. Zare, "Optimal bidding and offering strategies of merchant compressed air energy storage in deregulated electricity market using robust optimization approach," Energy, Vol. 142, 2018.

[18] S. Nojavan, M. Majidi, and K. Zare, "Risk-based optimal performance of a PV/fuel cell/battery/grid hybrid energy system using information gap decision theory in the presence of demand response program," Int. J. Hydrogen Energy, Vol. 42, No. 16, 2017.

[19] G. S. Piperagkas, A. G. Anastasiadis, and N. D. Hatziargyriou, "Stochastic PSO-based heat and power dispatch under environmental constraints incorporating CHP and wind power units," Electr. Power Syst. Res., Vol. 81, No. 1, 2011.

[20] T. Niknam, A. Kavousifard, S. Tabatabaei, and J. Aghaei, "Optimal operation management of fuel cell/wind/photovoltaic power sources connected to distribution networks," J. Power Sources, Vol. 196, No. 20, 2011.

[21] A. Najafi-Ghalelou, S. Nojavan, and K. Zare, "Heating and power hub models for robust performance of smart building using information gap decision theory," Int. J. Electr. Power Energy Syst., Vol. 98, 2018.

[22] S. Nojavan, H. Qesmati, K. Zare, and H. Seyyedi, "Large Consumer Electricity Acquisition Considering Time-of-Use Rates Demand Response Programs," Arab. J. Sci. Eng., Vol. 39, No. 12,2014.

[23] S. Nojavan, K. Zare, and M. R. Feyzi, "Optimal bidding strategy of generation station in power market using information gap decision theory (IGDT)," Electr. Power Syst. Res., Vol. 96, 2013.

[24] A. Najafi-Ghalelou, S. Nojavan, and K. Zare, "Information gap decision theory-based risk-constrained scheduling of smart home energy consumption in the presence of solar thermal storage system," Sol. Energy, Vol. 163, 2018.